Stable topological textures in a classical two-dimensional Heisenberg model

E. G. Galkina,[1] E. V. Kirichenko,[2] B. A. Ivanov,[3,4,*] and V. A. Stephanovich[2,†]
[1]*Institute of Physics, 03028 Kiev, Ukraine*
[2]*Opole University, Institute of Mathematics and Informatics, Opole 45-052, Poland*
[3]*Institute of Magnetism, 03142 Kiev, Ukraine*
[4]*National T. Shevchenko University of Kiev, 03127 Kiev, Ukraine*
(Received 17 January 2009; revised manuscript received 27 March 2009; published 30 April 2009)

We show that stable localized topological soliton textures (skyrmions) with π_2 topological charge $\nu \geq 1$ exist in a classical two-dimensional Heisenberg model of a ferromagnet with uniaxial anisotropy. For this model the soliton exists only if the number of bound magnons exceeds some threshold value N_{cr} depending on ν and the effective anisotropy constant K_{eff}. We define soliton phase diagram as the dependence of threshold energies and bound magnons number on anisotropy constant. The phase boundary lines are monotonous for both $\nu=1$ and $\nu>2$ while the solitons with $\nu=2$ reveal peculiar nonmonotonous behavior, determining the transition regime from low to high topological charges. In particular, the soliton energy per topological charge (topological energy density) achieves a minimum neither for $\nu=1$ nor high charges but rather for intermediate values $\nu=2$ or $\nu=3$. We show that this peculiarity is related to the character of convergence of integrals defining soliton energy and number of bound magnons at different ν.

DOI: 10.1103/PhysRevB.79.134439 PACS number(s): 75.10.Hk, 75.30.Ds, 05.45.−a

I. INTRODUCTION

The studies of nonlinear excitations of two-dimensional (2D) and quasi-2D correlated spin systems are an important issue of modern physics of magnetism, and can be useful for development of general soliton concepts.[1–6] The topological textures such as localized solitons (skyrmions[7]) or magnetic vortices make an important contribution to the thermodynamics of magnetically ordered systems,[8] or even determine the character of its ordering as in the case of Berezinskii-Kosterlitz-Thouless transition.[9,10] In recent years the interest for two-dimensional solitons has grown since they are frequently realized as ground state in the finite-size mesoscopic magnetic samples, so-called magnetic dots.[11] Skyrmions and other types of topological excitations appear not only in physics of magnetism but in other branches of physics. Namely, 2D soliton textures have been subject of intensive studies in mathematical physics,[12] theoretical condensed-matter physics (e.g., in Ginzburg-Landau theory of superconductivity[13,14]), as well as in some astrophysical models (see, e.g., Ref. 15, and references therein). The questions of dynamics and stability of one-dimensional (1D) solitons have been considered in Refs. 16–18.

The most "famous" topological solitons are magnetic vortices having π_1 topological charge. These vortices are usually related to thermodynamic aspects of soliton physics.[9,10] Also, they appear in mesoscopic nanostructures.[11] Easy-plane magnets with continuously degenerated ground state have vortices with the energy being logarithmically divergent as a function of system size. The other and much less studied example of topological solitons is magnetic skyrmions which are present in isotropic or easy-axis magnets. Contrary to the above vortices, the latter textures are characterized by nontrivial π_2 topological charge and finite energy. It is known that they determine the response functions of 2D magnets at finite temperatures[19,20] and take part in long-range order breakdown in isotropic magnets.[21] The skyrmions form ground state of magnetic nanoparticles with easy-axis anisotropy.[22] Their analysis is more complicated as compared to magnetic vortices and comprises many nontrivial features. An important example of latter features is the problem of a skyrmion stability since due to Hobart-Derrick theorem the static solitons with finite energy are unstable for wide class of models including standard continuous magnetic models.[23,24]

For magnetic vortices, the consideration of lowest possible topological charge $\nu=1$ is sufficient as the vortex energy grows with ν, $E_\nu^{\text{vort}} \propto \nu^2$. Because of that it is advantageous for a vortex with $\nu>1$ to decay for ν vortices with $\nu=1$ and the vortices with $\nu=2$ can be stable in exceptional cases only.[25] The situation for skyrmions is not that simple. The simplest continuous model for isotropic 2D ferromagnet (FM),

$$W^{\text{is}} = \frac{Ja^2S^2}{2}\int [\nabla \vec{m}]^2 d^2x, \tag{1}$$

admits the well-known Belvin-Polakov (BP) solution,[21] which reads

$$\tan\frac{\theta}{2} = \left(\frac{R}{r}\right)^{\nu}, \quad \varphi = \varphi_0 + \nu\chi, \tag{2}$$

where $\vec{m}$ is normalized magnetization

$$\vec{m} = (\sin\theta\cos\varphi; \sin\theta\sin\varphi; \cos\theta), \tag{3}$$

S is a spin value, a is a lattice constant of a 2D FM, J is its exchange constant, r and χ are polar coordinates in the XY plane, and φ_0 is an arbitrary constant. Solution (2) has the energy

$$E_{0\nu} = \nu E_0, \quad E_0 = 4\pi JS^2, \tag{4}$$

so that the state of BP skyrmions with $\nu>1$ merges or dissociates into several other similar skyrmions with different ν's (the only rule that in such process the topological charge

should conserve) without their energy altering. Such exact degeneration is related to very high hidden symmetry, stemming from exact integrability of corresponding static model (1) (see, e.g., Ref. 21). This degeneration should certainly be lifted if we go beyond the model (1). The most important characteristic here is the parameter $\mathcal{E}_\nu$, which is appropriate to call the *topological energy density*,

$$\mathcal{E}_\nu = \frac{E_\nu}{\nu}, \tag{5}$$

where E_ν is the energy of a soliton with topological charge ν. If $\mathcal{E}_\nu$ is a growing function of ν, the most favorable state with a given ν comprises ν solitons with unit topological charge; otherwise such state is unstable. Latter question is especially important for the investigation of general regularities of the highly excited magnet state evolution, (see, e.g., Ref. 26 and references therein) or for the analysis of essentially inhomogeneous magnet states under strong pumping.[27] Latter states can be generated by the ultrafast pulses of magnetic field, see Refs. 28 and 29 for details. The preceding discussion demonstrates that the problem of obtaining and investigation of the stable skyrmions with higher topological charges is extremely important.[30]

The present work is devoted to the analysis of skyrmions with higher π_2 topological charges in 2D Heisenberg ferromagnet with uniaxial anisotropy [Eq. (6)]. We show that there exists a certain range of system parameters (exchange and anisotropy constants) where stable precessional solitons with topological charge $\nu>1$ exist. It turns out that, in wide range of anisotropy constants, the topological energy density $\mathcal{E}_\nu$ of the textures with $\nu>1$ is lower than that of the textures with $\nu=1$. On the other hand, the solitons with $\nu=1$ and $\nu>2$ have monotonously growing phase boundary functions $\mathcal{E}_{\nu,\mathrm{cr}}(N_{\nu,\mathrm{cr}})$ while the case $\nu=2$ has peculiar nonmonotonous behavior, determining the transition regime from low to high topological charges. This means that the preferable values of soliton topological charge are neither $\nu=1$ nor high charges but rather $\nu=2$ or $\nu=3$.

II. MODEL DESCRIPTION AND SOLITON CLASSIFICATION

We begin with the discrete model of a classical 2D FM with uniaxial anisotropy, described by the following Hamiltonian

$$\mathcal{H} = -\frac{1}{2}\sum_{\vec{n},\vec{a}} (J\vec{S}_{\vec{n}}\cdot\vec{S}_{\vec{n}+\vec{a}} + \kappa S^z_{\vec{n}} S^z_{\vec{n}+\vec{a}}) + K\sum_{\vec{n}} [(S^x_{\vec{n}})^2 + (S^y_{\vec{n}})^2]. \tag{6}$$

Here $\vec{S}\equiv(S^x,S^y,S^z)$ is a classical spin vector with fixed length S on the site $\vec{n}$ of a 2D square lattice. The summations run over all lattice sites $\vec{n}$ and nearest-neighbors $\vec{a}$, $J>0$ is the exchange integral, and the constant κ describes the anisotropy of spin interaction. In subsequent discussion, we refer to this type of anisotropy as exchange anisotropy (EA). Additionally, we took into account single-ion anisotropy (SIA) with constant K. We consider z axis to be easy magnetization direction so that $K>0$ or $\kappa>0$.

The analysis of real magnetic systems with discreet spins can be performed only numerically. In principle, it can be done by the same method as was described in Ref. 31 but it is not easy to extract necessary information from the set of numerical data. On the other hand, if we neglect the specific effects of discreteness (which appear at strong anisotropy only, K, $\kappa\geq J$), such as the presence of pure collinear structures,[31] the consideration can be simplified using the continuous approximation and classical Landau-Lifshitz equations. In this approximation we can introduce the smooth function $\vec{S}(x,y,t)$ instead of discreet variable $\vec{S}_n(t)$. In this case, the classical magnetic energy functional $W[\vec{S}]$ can be constructed expanding the discrete Hamiltonian (6) in power series of magnetization gradients, yielding

$$E_\nu = W_2 + W_4 + \cdots, \tag{7}$$

where W_2 contains zeroth and second-order contributions to magnetic energy, see Eq. (1), and W_4 contains the fourth powers of gradients. The explicit expressions for W_2 and W_4 read

$$W_2 = \int d^2x \left\{ \frac{K_{\mathrm{eff}}}{a^2}(S^2 - S_z^2) + \frac{J}{2}(\nabla\vec{S})^2 + \frac{\kappa}{2}(\nabla S_z)^2 \right\}, \tag{8a}$$

$$W_4 = -\frac{a^4}{24}\int d^2x \left\{ J\left[\left(\frac{\partial^2\vec{S}}{\partial x^2}\right)^2 + \left(\frac{\partial^2\vec{S}}{\partial y^2}\right)^2 \right] + \kappa\left[\left(\frac{\partial^2 S_z}{\partial x^2}\right)^2 + \left(\frac{\partial^2 S_z}{\partial y^2}\right)^2 \right] \right\}, \tag{8b}$$

where ∇ is a 2D gradient of the function $\vec{S}(\vec{r},t)$. Here, we used integrations by parts with respect to the fact that our soliton texture is spatially localized. Also, we introduce the effective anisotropy constant

$$K_{\mathrm{eff}} = K + 2\kappa. \tag{9}$$

We note here that single-ion anisotropy enters only W_2 but not W_4 and higher terms while exchange anisotropy enters every term of the expansion (7). In the angular variables (3) the expression for the classical magnetic energy (7) assumes the form

$$E[\theta,\phi] = W_2 + W_4, W_2 = S^2\int d^2x \left\{ \frac{K_{\mathrm{eff}}}{a^2}\sin^2\theta + \frac{1}{2}[(\nabla\theta)^2(J+\kappa\sin^2\theta) + J(\nabla\varphi)^2\sin^2\theta] \right\},$$

$$W_4 = -\frac{1}{24}a^2S^2\int d^2x\{(\nabla^2\theta)^2[J+\kappa\sin^2\theta] + (\nabla\theta)^4[J + \kappa\cos^2\theta] + J\sin^2\theta(\nabla\varphi)^2[(\nabla\varphi)^2 + 2(\nabla\theta)^2] + 2\sin\theta\cos\theta(\nabla^2\theta)[\kappa(\nabla\theta)^2 - J(\nabla\varphi)^2]\}. \tag{10}$$

For isotropic case $K=0$ and $\kappa=0$, W_2 coincides with the energy of the isotropic continuous model (1) bearing BP soliton solutions of the form (2) with degenerate (with respect to

topological charge) topological energy density (5), see also Eq. (4). A simple accounting of magnetic anisotropy in W_2 generates a model, which is typical example of the models governed by Hobart-Derrick theorem—it does not admit static stable soliton solutions. In the model with $W=W_2$ only, the size of any texture such as domain wall, soliton, etc. (see, e.g., Ref. 31 for details) is given by the characteristic length l_0

$$l_0^2 = \frac{a^2 J}{2K_{\text{eff}}}. \tag{11}$$

In the case of weak anisotropy, $K_{\text{eff}} \ll J$, the length scale $l_0 \gg a$ so that the magnetization varies slowly in a space.

Now we consider generalized model (7), including higher powers of gradients. Here we note that the entire expansion of the energy E_ν in powers of magnetization gradients will be sign alternating with a negative sign of the coefficient before fourth order derivatives [Eq. (8)]. Formally, a continuum theory like this is unstable because the system can minimize the energy infinitely by creating more and more magnetization gradients. Below we will demonstrate that such instability does not occur in our model since it would take place for regimes $l_0 < a$ where the gradient expansion is not valid. In other words, the inequality $l_0 < a$ corresponds to the case of strong magnetization inhomogeneities at distances smaller than lattice spacing a, where phenomenological description is invalid.

In the expansion (7), we limit ourselves to the terms of fourth order only as they are playing a decisive role in soliton stabilization, see Refs. 32 and 33 for details. The simplest possible generalized model with account for W_4 only can in principle admit the above static stable solitons.[2] Simple scaling arguments can demonstrate that. Namely, if a skyrmion texture has localization radius R, the simple estimations yield the dependence of the energy E_ν on R in the form

$$E_\nu = -A_\nu \frac{l_0^2}{R^2} + B_\nu + C_\nu \frac{R^2}{l_0^2}, \tag{12}$$

where the first term comes from W_4 and the rest come from W_2. If $E_\nu(R)$ had a minimum (this occurs if $A_\nu < 0$), this would mean the existence of a stable static skyrmion. Unfortunately, for the real model of magnet [Eq. (6)] $A_\nu > 0$ so that the first term is negative and the dependence $E_\nu(R)$ does not have a minimum. We note also that the expansion (7) and the above scale arguments are valid for any symmetry of initial 2D discrete lattice. The only difference is in the coefficients before gradient powers. Although these coefficients influence the soliton properties, the main feature of these expansions, consisting of the fact that in Eq. (12) $A_\nu > 0$ remains the same. In other words, we did not find any symmetry of 2D FM with nearest-neighbor ferromagnetic interaction, where $E_\nu(R)$ has a minimum so that stable static soliton can exist.[34]

In the absence of *static* two-dimensional solitons, it is possible to construct stable soliton states with *stationary dynamics* due to the presence of additional integrals of motion for magnetization fields. The purely uniaxial model (6) possesses the exact symmetry with respect to the spin rotation around z axis so that the energy functional $E_\nu[\theta, \varphi]$ does not depend explicitly on the variable φ. This leads to the appearance of an additional integral of motion: z projection of total spin. This integral of motion can be conveniently parametrized via integer N defining a number of bound magnons in a soliton N, see Ref. 5 for details. In continuous approximation it can be written as

$$N = \frac{S}{a^2} \int d^2x (1 - \cos\,\theta). \tag{13}$$

Conservation of N leads to the presence of so-called *precessional* solitons characterized by time-independent projection of magnetization onto the easy z axis and with the precession of the magnetization vector $\vec{m}$ at constant frequency ω around the z axis,

$$\theta = \theta(r), \varphi = \omega t + \nu\chi + \varphi_0, \tag{14}$$

which holds instead of Eq. (2) in this case. The analogs of such precessional solitons are known to occur in different field-theoretical models; it is enough to note the nontopological Coleman's Q balls,[35] which do not have topological properties as well as π_2 topological Q lumps,[36] see Ref. 2 for details.

Stable dynamical solutions with nonzero ω correspond to conditional (for fixed N value) minimum of the energy functional E_ν. Namely, we may look for an extremum of the expression

$$L = E_\nu - \hbar\omega N, \tag{15}$$

where ω is an internal soliton precession frequency, which in this case can be regarded as Lagrange multiplier. Note that functional (15) is nothing but the Lagrangian of 2D FM magnetization field calculated with respect to specific time dependence (14). This condition leads to the relation[5] $\hbar\omega = dE_\nu/dN$, which determines the microscopic origin of the precessional frequency ω. Namely, an addition of one extra spin deviation (bound magnon) to a soliton changes its energy by $\hbar\omega$. Thus, the dependencies $E_\nu(N)$ and $\omega(N)$ are very important for the problem of a soliton stability.

III. STRUCTURE AND STABILITY OF SKYRMIONS AND CRITICAL ENERGY

Further analysis of above continuous model consists of the solution of differential equations for soliton structure, which is equivalent to the minimization of the functional (7). As these equations can barely be solved analytically, here we analyze the soliton properties by direct variational method. As we have shown earlier by comparison of variational approach and direct numerical minimization of initial discreet energy on a lattice,[31] the variational approach gives fairly good results for weak anisotropies $K_{\text{eff}} \leq 0.5J$, where the generalized continuous description is valid.

The continuous models such as Eqs. (1) and (7) are usually parametrized by angular variable (3) so that the energy E_ν becomes a functional of these variables, $E_\nu \equiv E_\nu[\theta, \nabla\theta, \phi, \nabla\phi]$. Having energy functional E_ν, we can write the corresponding Landau-Lifshitz equations and Lagrangian (15).

To apply direct variational method for minimization of the energy $E_\nu = W_2 + W_4$, we use the trial function

$$\tan\frac{\theta}{2} = \frac{2^{1-\nu}(\Lambda R)^\nu}{(\nu-1)!}K_\nu(\Lambda r), \tag{16}$$

where $K_\nu(x)$ is the McDonald function with index ν.[37] Note that trial function (16) is based on the interpolative solution, constructed in Ref. 38. The trial function (16) gives correct asymptotics both for $r \to 0$ (corresponding to BP soliton) and for $r \to \infty$ (exponential decay with some characteristic scale $1/\Lambda$), see Refs. 5, 32, and 38 for details. Latter exponential asymptotics is absent for solitons in isotropic 2D FM, e.g., for BP soliton [Eq. (2)]. It can be shown that the exponential asymptotics occurs for anisotropic models, where the length of decay is proportional to l_0 [Eq. (11)]. It had been demonstrated that, due to power-law asymptotics of $\theta(r)$ for isotropic magnet, the integrals defining soliton energy and number of bound magnons [see below Eq. (21)] are divergent for $\nu = 1$.[5,32,38] To avoid this divergency in anisotropic models such as Eq. (6), the interpolative (between BP asymptotics at $r \to 0$ and exponential one at $r \to \infty$) solution had been put forward in Ref. 38. Our analysis of continuous model (7) shows that at $\nu = 1$ the above divergence can be cutoff by the exponential asymptotics only. For $\nu = 2$ the power-law asymptotics is sufficient for convergence of corresponding integrals while their derivatives with respect to parameter Λ are divergent. In this case, the divergences in derivatives are also eliminated by exponential asymptotics. At $\nu > 2$ all integrals and their derivatives (with respect to Λ) are convergent. This means that the behavior of solitons with $\nu = 1$ and 2 on one side, and those with $\nu > 2$ on the other side is different, being determined by the interplay between effects of anisotropy and higher spatial derivatives.

In our minimization method, the parameter Λ is variational while the parameter R is kept constant as it is related to N, $N \propto R^2$, see, e.g. Ref. 5. In other words, we minimize the energy E with trial function (16) over Λ for constant R. This approach has the advantage that it also permits investigating of the stability of obtained soliton texture. Namely, a soliton is stable if it corresponds to the conditional minimum of the energy at fixed N, and it is unstable otherwise.

To proceed further, we introduce following dimensionless variables

$$x = \Lambda r, \quad \lambda = a\Lambda, \quad z = \Lambda R, \tag{17}$$

and express trial function (16) in terms of them. We have

$$\tan\frac{\theta}{2} = \frac{2^{1-\nu}z^\nu}{(\nu-1)!}K_\nu(x). \tag{18}$$

Then using Eq. (13), we can calculate the number of bound magnons in the soliton

$$\frac{N}{S} = \frac{2\pi}{\lambda^2}\int_0^\infty (1-\cos\theta)xdx \equiv \frac{2\pi}{\lambda^2}\psi(z). \tag{19}$$

In variables (17) the soliton energy assumes the form

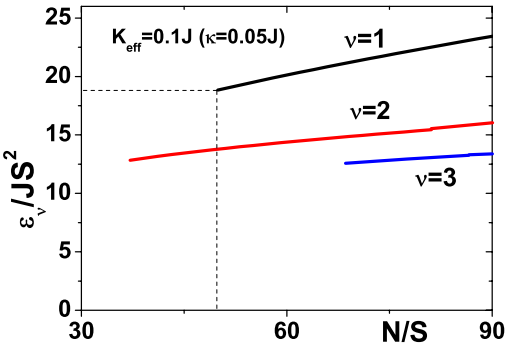

FIG. 1. (Color online) Dependence of a soliton topological energy density $\mathcal{E}_\nu(N)$ for skyrmions with different ν's and exchange anisotropy only, $\kappa = 0.05J$ ($K_{\text{eff}} = 0.1J$). Dashed lines show $\mathcal{E}_{\nu,\text{cr}}(\nu)$ and $N_{\nu,\text{cr}}$ for $\nu = 1$.

$$\frac{\mathcal{E}_\nu}{2\pi JS^2} = \frac{K_{\text{eff}}}{\lambda^2}\gamma_0(z) + \gamma_2(z) - \frac{1}{24}\lambda^2\gamma_4(z), \tag{20}$$

where

$$\gamma_0(z) = \int_0^\infty \sin^2\theta xdx,$$

$$\gamma_2(z) = \frac{1}{2}\int_0^\infty xdx\left[\theta'^2(1+\kappa\sin^2\theta) + \frac{\nu^2\sin^2\theta}{x^2}\right],$$

$$\gamma_4(z) = \int_0^\infty xdx\left\{(\Delta_x\theta)^2(1+\kappa\sin^2\theta) + \theta'^4(1+\kappa\cos^2\theta) + \frac{\nu^2\sin^2\theta}{x^2}\left(\frac{\nu^2}{x^2} + 2\theta'^2\right) + \Delta_x\theta\sin 2\theta\left(\kappa\theta'^2 - \frac{\nu^2}{x^2}\right)\right\},$$

$$\theta' = \frac{d\theta}{dx}, \quad \Delta_x\theta = \frac{d^2\theta}{dx^2} + \frac{1}{x}\frac{d\theta}{dx}. \tag{21}$$

Thus, we express the energy and the number of magnons via two parameters, λ and z. It turns out that initial dimensional variables Λ and R enter the problem only in the form of their product z. The dependence of N and E_ν on z enters the problem via a few complicated functions ψ, γ_0, γ_2, and γ_4, which can be written only implicitly in the form of integral (21). However, in terms of these functions, the dependence on λ [Eq. (20)] turns out to be quite simple. This permits reformulation of the initial variational problem in terms of variables z and N only. Namely, we express

$$\lambda^2 = \frac{2\pi}{(N/S)}\psi(z), \tag{22}$$

and substitute this expression into the dimensionless energy [Eq. (20)]. This gives us the expression for the energy of a soliton with given N, as a function of variational parameter z. Then we can find a minimum of E_ν with respect to z, keeping N constant.

The result of such numerical minimization in the form of the dependence $\mathcal{E}_\nu(N)$ is shown in Fig. 1 for a magnet with purely exchange anisotropy $\kappa = 0.05$. The curves for higher κ are qualitatively the same. To justify the applicability of our

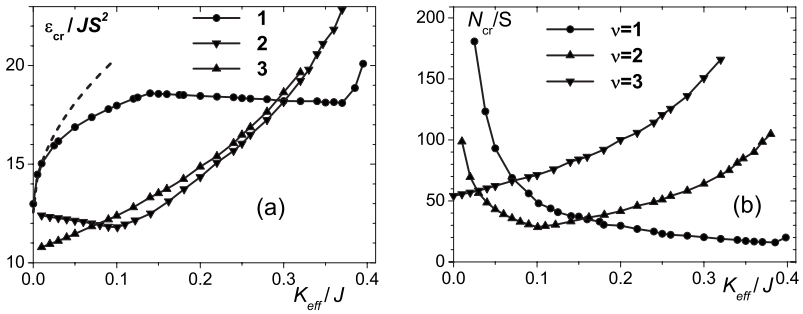

FIG. 2. Soliton phase diagram. (a) Threshold topological energy density [dashed line at small K_{eff} is described by Eq. (27)], (b) Threshold magnon number. Solitons exist at $\mathcal{E}>\mathcal{E}_{\text{cr}}$ and $N>N_{\text{cr}}$. For small κ the value of N_{cr} is divergent as $1/\sqrt{K_{\text{eff}}}$ at $\nu=1$ and 2, and is constant at $\nu\geq 3$.

direct variational approach, earlier we have shown[31] that for $\nu=1$ the dependencies $\mathcal{E}_\nu(N)$ found by variational and numerical minimizations of the energy are identical at small enough anisotropy, $K_{\text{eff}}\leq 0.5J$.

Our analysis shows (see also Fig. 1) that topological energy density grows slowly as function of N. We note here that this property holds for all anisotropy constants and topological charges. Even more interesting is the fact that all curves $\mathcal{E}_\nu(N)$ have threshold points $\mathcal{E}_{\nu,\text{cr}}=\mathcal{E}_\nu(N_{\nu,\text{cr}})$ so that solitons exist only at $\mathcal{E}_\nu>\mathcal{E}_{\nu,\text{cr}}$ and $N_\nu>N_{\nu,\text{cr}}$. These threshold values determine the minimal soliton energy, which is most important characteristic of soliton contribution into magnet thermodynamics and can be observed experimentally.[19] For instance (see Fig. 1), at $\nu=1$ and $\kappa=0.05J$ $\mathcal{E}_{\nu,\text{cr}}\approx 18JS^2$, which is substantially higher than that expected from Eq. (4) $4\pi JS^2\approx 12.56JS^2$.

Figure 1 demonstrates one more unexpected soliton property, namely, that at $\kappa=0.05J$ the energy density $\mathcal{E}_\nu(N)$ *decreases* with increase in ν and fixed N value. As we will show below, such behavior occurs for many values of K_{eff} although there can be exceptions. The most important feature, however, is the existence of above threshold energy and bound magnon number values. The behavior of these values at variation in anisotropy constants is quite nontrivial. For example, at $\kappa=0.05J$ (the value chosen for Fig. 1) $N_{\text{cr}}(\nu=1)>N_{\text{cr}}(\nu=2)$ but $N_{\text{cr}}(\nu=3)>N_{\text{cr}}(\nu=1)$. At the same time, the corresponding threshold energies behave monotonically $\mathcal{E}_{\text{cr}}(\nu=1)>\mathcal{E}_{\text{cr}}(\nu=2)>\mathcal{E}_{\text{cr}}(\nu=3)$. Our extensive analysis of numerical curves $\mathcal{E}_\nu(N)$ for different anisotropies has shown that their overall behavior is dictated primarily by the threshold values: if $\mathcal{E}_{\nu,\text{cr}}>\mathcal{E}_{\nu',\text{cr}}$, then the entire curve $\mathcal{E}_\nu(N)$ lies above corresponding curve $\mathcal{E}_{\nu'}(N)$ in wide interval of N's. This shows the importance of the above threshold values for the properties of solitons. The information about these values can be conveniently represented in the form of so-called soliton phase diagram, i.e., the dependence of $\mathcal{E}_{\text{cr}}$ and N_{cr} on K_{eff}.

IV. SOLITON PHASE DIAGRAM

To obtain the phase diagram, we should pay attention to the details of above minimization procedure. Namely, to obtain truly stable soliton texture we should demand that the conditional extremum of the energy E_ν is a minimum. So, we keep track not only to the first derivative dE_ν/dz to be zero but also to the second derivative to be positive (corresponding to a minimum) at the point $z_{\min}$, where $dE_\nu/dz=0$. When a soliton approaches the limit of its stability, the modulus of second derivative diminishes, becoming zero at the stability limit z_{cr}, corresponding to above values $\mathcal{E}_\nu\equiv\mathcal{E}_{\nu,\text{cr}}$ and $N=N_{\nu,\text{cr}}$. Thus the above soliton phase diagram is indeed determined by the instability point z_{cr} (as a function of ratio K_{eff}/J) where both first and second derivatives of the energy are zero.

The shape of the above phase diagram is determined by the character of anisotropy and ν value, and is reported on Fig. 2 for exchange anisotropy. First of all, one can see that the dependence $\mathcal{E}_{\text{cr}}(\nu)$ is quite complicated and its character changes twice, at $K_{\text{eff}}\approx 0.07$ and at $K_{\text{eff}}\approx 0.29$. It is seen from Fig. 2(a) that, while there is a quite large region of K_{eff} values, where $\mathcal{E}_2$ and $\mathcal{E}_3$ are smaller than $\mathcal{E}_1$, the region where $\mathcal{E}_3<\mathcal{E}_2$ is approximately three times smaller. We have shown that $\mathcal{E}_4$ is always larger than $\mathcal{E}_3$ although still smaller than $\mathcal{E}_1$. The energy $\mathcal{E}_{\text{cr}}(\nu)$ is growing with ν at $K_{\text{eff}}\geq 0.29J$ only.

Figure 2(b) demonstrates the divergence of N_{cr} at small K_{eff} as $\nu=1$ and 2. This is related to the fact that in BP soliton the integral describing N diverges logarithmically as $r\to\infty$ for $\nu=1$, see also above.

Overall, Fig. 2 demonstrates the complicated behavior of soliton phase diagram, which is needed to be understood. To understand better the above complex behavior, it is instructive to obtain the phase diagram analytically. Without loss of generality, we shall do so for the case of uniaxial anisotropy only. Such analytical treatment is possible since the anisotropy constant K in this case enters the problem only via coefficient in the first term of Eq. (20). This permits obtaining of the analytic dependencies $\mathcal{E}_{\nu,\text{cr}}(K)$ and $N_{\nu,\text{cr}}(K)$ in the inverse form $K(\mathcal{E},N)$. Note that the structure of Eq. (21) suggests that the above analytical procedure is applicable for both exchange and uniaxial anisotropies. Our analysis shows that this does not change the situation qualitatively. Moreover, the quantitative results are close to each other, compare Figs. 2 and 4.

As it was shown above, the soliton phase diagram is determined by the instability point z_{cr}. To obtain an equation for latter point, we rewrite Eq. (20) in the form

$$\frac{\mathcal{E}_\nu}{2\pi JS^2}=a(z)y+b(z)-\frac{c(z)}{y},$$

$$y=\frac{N}{S},\quad a(z)=\frac{K\gamma_0(z)}{2\pi J\psi(z)},$$

$$b(z)=\gamma_2(z),\quad c(z)=\frac{\pi}{12}\gamma_4(z)\psi(z), \tag{23}$$

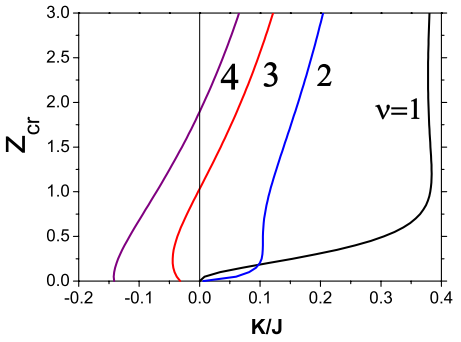

FIG. 3. (Color online) Dependence $z_{\rm cr}(K/J)$. Numbers near the curves correspond to ν values.

[function $\psi(z)$ is defined by Eq. (19)] and equate to zero the first and second derivatives of $\mathcal{E}_\nu$ with respect to z. This gives the equation for the dependence $y(z_{\rm cr})$ in the form

$$y_{\rm cr} \equiv y(z_{\rm cr}) = -\frac{b'(z_{\rm cr})c''(z_{\rm cr}) - c'(z_{\rm cr})b''(z_{\rm cr})}{a'(z_{\rm cr})c''(z_{\rm cr}) - c'(z_{\rm cr})a''(z_{\rm cr})}, \qquad (24)$$

where primes mean corresponding derivatives. Then, the equation for $z_{\rm cr}$ can be obtained by substitution of above $y_{\rm cr}$ into one of the equations determining zero for first or second energy derivatives with respect to z. It turns out that this equation always has real solutions if we formally admit the existence of negative K.

Dependence (24) permits obtaining of the equation for the phase diagram in the implicit form $K(z_{\rm cr})$, which reads

$$K(z_{\rm cr}) = \frac{J}{c''(z_{\rm cr})}\left[\frac{q''(z_{\rm cr})}{\pi}y_{\rm cr}^2 + b''(z_{\rm cr})y_{\rm cr}\right],$$

$$q(z) = \frac{\gamma_0(z)}{2\psi(z)}. \qquad (25)$$

The dependence $z_{\rm cr}(K)$, obtained by inversion of Eq. (25), is reported on Fig. 3. It is seen that, while the entire curves $z_{\rm cr}(K)$ at $\nu=1$ and 2 lie at $K>0$, the curves for $\nu>2$ lie in this range only partially. Since for uniaxial anisotropy K can be only positive, only those parts of the curves with $\nu>2$, where $K>0$ correspond to physically realizable case. This clarifies the reason why the dependence $N_{\rm cr}(K/J)$ for skyrmions with $\nu>2$ begins from finite N values, see Fig. 2(b). This different behavior is related to the different kinds of convergence of corresponding integrals at $\nu=1$ and 2 as well as for $\nu>2$, see discussion above.

The dependence $z_{\rm cr}(K/J)$ can be easily recalculated to the soliton phase diagram $\mathcal{E}_{{\rm cr}\nu}(K/J)$ and $N_{\rm cr}(K/J)$. This diagram is shown on Figs. 4(a) and 4(b). It is seen as the qualitative coincidence with the numerical curves from Figs. 2(a) and 2(b). The details of behavior can now be better seen than from above numerical curves.

Our analysis shows that aforementioned different character of convergence of integrals influences asymptotics of the phase diagram curves at small anisotropies. This influence can be seen from Figs. 2(a) and 4, where the dependence $\mathcal{E}_{\nu,{\rm cr}}(K/J)$ at $\nu=1$ and 2 is nonanalytical at $(K/J)\to 0$ while for $\nu>2$ it is analytical. The reason for such behavior can be seen from Fig. 3, showing that small K/J correspond to small z for $\nu=1$ and 2, while for $\nu>2$ all values of K/J including limiting case $K/J\to 0$ correspond to finite z. This means that at $\nu>2$ the asymptotic analysis of the curves $\mathcal{E}_{\nu,{\rm cr}}(K/J)$ can be done simply by Taylor expansion at small K/J, which yields simple monotonic behavior of $\mathcal{E}_{\nu,{\rm cr}}$ and $N_{\nu,{\rm cr}}$.

At $\nu=1$ and 2 the situation is not so simple and requires more complicated analysis. Such analysis can be performed on the base of Eqs. (24) and (25), and is quite cumbersome. The main idea is that functions $a(z)$, $b(z)$, and $c(z)$ in Eq. (23) at small z can be represented via exponential integral functions,[37] which, in turn, may be expanded in asymptotic series. This procedure for $\nu=1$ gives following parametric dependence

$$\frac{K}{J} = \frac{18}{\ln 3}z^4 \ln^6 z, \frac{\mathcal{E}_{\rm cr}}{4\pi JS^2} = 1 + \frac{4}{\ln 3}z^2 \ln^4 z,$$

$$\frac{N_{\rm cr}}{S} = \frac{4\pi}{9}\frac{1}{z^2 \ln^2 z}. \qquad (26)$$

Asymptotics (26) is shown by dashed line on Fig. 4(a). In the main logarithmic approximation this gives simple relations

$$\mathcal{E}_{1,{\rm cr}} = 4\pi JS^2(1 + C_1\sqrt{K/J}), \qquad (27)$$

$$N_{1,{\rm cr}} = \frac{SC_2}{\sqrt{K/J}}, \qquad (28)$$

which coincide with the results obtained in Ref. 31 by direct numerical modeling of the discreet model, giving $C_1 \approx 1.87$ and $C_2 \approx 5.65$.

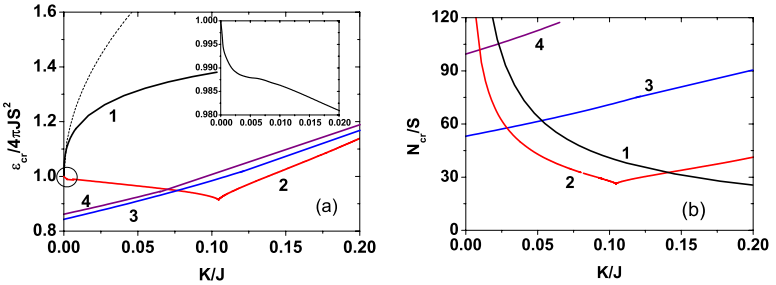

FIG. 4. (Color online) Soliton phase diagram for the model with uniaxial anisotropy only. (a) Threshold topological energy density [dashed line at small K/J is asymptotics (26)]. The inset expands the encircled area on the main panel and shows the behavior of $\mathcal{E}_{2,{\rm cr}}$ at small K/J. (b) Threshold magnon number. The ranges where solitons exist are similar to those on Fig. 2. Numbers near curves correspond to ν values.

These expressions give us an idea about behavior of energy and bound magnons number at small K. Namely, we see that the energy has the (approximate) square-root singularity while magnon number N obeys inverse square-root law. Asymptotics (27) is shown on Fig. 4(a) by dashed line.

For $\nu=2$ the same approximation gives

$$\frac{K}{J} = \frac{0.006\,648\,2}{\ln^2 z} + \frac{0.013\,220\,7z}{\ln^2 z},$$

$$\frac{N_{\rm cr}}{S} = -187.047 \ln z - 108.007,$$

$$\frac{\mathcal{E}_{\rm cr}}{4\pi JS^2} = 1 + \frac{0.027\,62}{\ln z} + \frac{0.015\,95}{\ln^2 z}. \qquad (29)$$

This also yields the divergent $N_{2,\rm cr}(K)$ and square-root peculiarity in the energy $\mathcal{E}_{2,\rm cr}(K)$. However, the coefficient before $\sqrt{K/J}$ in the energy is much smaller than that at $\nu=1$, which makes it almost invisible in the scale of Fig. 4. The details of this behavior are reported on the inset of Fig. 4(a).

This shows the similarities and differences between cases $\nu=1$ and $\nu=2$, which can also be seen from Fig. 4. Namely, if the topological energy densities for skyrmions with $\nu=1$ and 2 have both square-root nonanalyticity, for $\nu=2$ this nonanalyticity reveals only as a small cusp in a close vicinity of $K=0$. Other peculiarity of $\nu=2$ case is nonmonotonous behavior of $\mathcal{E}_{\rm cr2}$ (decreasing at $K<0.1J$ with subsequent increase). Our analysis shows that the above peculiarities of the skyrmion with $\nu=2$ are due to interplay between exponential asymptotics of $\theta(r)$, necessary to cut off the divergence at $\nu=1$ and 2 as well as power-law asymptotics, which is sufficient for the convergence at $\nu>2$.

V. DISCUSSION AND CONCLUDING REMARKS

In this paper we present a comprehensive theoretical study of the localized topological solitons (skyrmions), stabilized by precessional spin dynamics, for the classical 2D ferromagnet with easy-axial anisotropy on a square lattice. Our efforts were directed primarily toward the study of the role of higher π_2 topological charges $\nu>1$ on the above soliton properties. Our main conclusion is that the interplay between high topological charges, effects of lattice discreteness (in the form of higher powers of magnetization gradients), and uniaxial magnetic anisotropy makes many unexpected peculiarities into soliton properties as compared to those in the simplest isotropic continuous model with $W_4=0$, containing BP solitons.

Similar to previous studies, it turns out that the presence of even weak anisotropy makes solitons dynamic, i.e., those with nonzero precession frequency for any number N of bound magnons. The minimal consideration of discreteness (via higher degrees of gradients of magnetization) yields the existence of some threshold value of both soliton energy [topological energy density (5), which is more appropriate characteristic for solitons with $\nu>1$] and the number of bound magnons. Similar to the problem of cone state vortices,[33] the instability is related to the joint action of discreteness and anisotropy.

As a result, the critical values of bound magnons $N_{\nu,\rm cr}$ and soliton energy $\mathcal{E}_{\nu,\rm cr}$ is present, and nonanalytic dependencies of above threshold values on the anisotropy constant appear at $\nu=1$ and $\nu=2$. It was shown earlier[31] that the variational minimization of W_2 (i.e., energy, incorporating only squares of magnetization gradients) gives no threshold for soliton existence, i.e., the soliton exists everywhere up to $N=0$. This means that mapping of the initial discrete model even for small anisotropy $K_{\rm eff}\ll J$ on the simplest continuum model [Eq. (1)] is wrong, and to get the correct description of solitons in 2D FM we have to consider at least fourth powers of magnetization gradients. This seemingly paradoxical result is actually due to the fact that the terms with $(\nabla\vec{m})^2$ are scale invariant (so that the corresponding energy has a saddle point) while the (stable) soliton size is determined by the fourth derivatives as well as by a magnetic anisotropy. Our analysis shows that higher (than fourth) powers of magnetization gradients do not change the situation qualitatively, rather, in the range of above-studied $K_{\rm eff}$ these terms make only a small quantitative contribution to the soliton phase diagram. This means that solitons with $\nu=1$ can be well studied within the model (7). Earlier,[32,39] this model had been applied to study the dynamics and stability of skyrmions in thin magnetic films. In the paper,[39] the dynamics of skyrmion is studied by means of Landau-Lifshitz equations with Hilbert relaxation term. Both papers[32,39] consider the influence of higher powers of magnetization gradients (due to effects of lattice discreteness) and anisotropy on the skyrmion texture stability.

In summary, we have shown the existence of stable topological π_2 solitons (skyrmions) in the 2D ferromagnet with uniaxial anisotropy on a square lattice. Since for any 2D lattice symmetry the structure of corresponding energy functional (12) is the same, we may speculate that such textures exist in any 2D magnet with uniaxial anisotropy. The main nontrivial and unexpected result of the paper is that, while the solitons with $\nu=1$ and $\nu>2$ have monotonously growing phase boundary functions $\mathcal{E}_{\nu,\rm cr}(N_{\nu,\rm cr})$, the case $\nu=2$ has peculiar nonmonotonous behavior, determining the transition regime from low to high topological charges. This means that the designated value of soliton topological charge, which is expected for highly excited state of FM, is neither $\nu=1$ nor high charges but rather $\nu=2$ or $\nu=3$. We show that the reason for above nontrivial behavior is a different character of the energy and magnon number integral convergence at $\nu\leq 2$ and $\nu>2$. Namely, at $\nu=1$ the isotropic BP solution [Eq. (2)] yields the divergent integrals. In this case, the convergence is ensured by the anisotropy-generated exponential asymptotics of the function $\theta(r)$ with the characteristic decay length l_0 [Eq. (11)]. On the contrary, for $\nu>2$ the genuine BP power-law asymptotics is sufficient for integrals to be convergent. Latter asymptotics is also peculiar to the generalized continuous model with account for higher powers of magnetization gradients, see Eq. (12). This means that at higher topological charges the soliton is stabilized by the higher-order

derivative terms while at $\nu=1$ the stabilization occurs by the anisotropy. Our analysis shows that at $\nu=2$ and $\nu=3$ the integral convergence is determined more or less equally by exponential (anisotropy-generated) and power-law (that is to say, higher-order derivative generated) asymptotics. This demonstrates the designated role of the cases $\nu=2$ and $\nu=3$ in soliton stabilization.

ACKNOWLEDGMENTS

This work was supported by Grant No. INTAS-05-1000008-8112, by joint Grant No. 219–08 from the Russian Foundation for Basic Research and Ukrainian Academy of Science, and by Opole University Intramural Grant (Badania Statutowe).

*bivanov@i.com.ua

†stef@math.uni.opole.pl; http://cs.uni.opole.pl/~stef

[1] T. Vachaspati, *Kinks and Domain Walls: An Introduction to Classical and Quantum Solitons* (Cambridge University Press, Cambridge, 2006).

[2] N. Manton and P. Sutcliffe, *Topological Solitons* (Cambridge University Press, Cambridge, 2004).

[3] A. P. Malozemoff and J. C. Slonczewski, *Magnetic Domain Walls in Bubble Materials* (Academic, New York, 1981).

[4] V. G. Bar'yakhtar, M. V. Chetkin, B. A. Ivanov, and S. N. Gadetskii, *Dynamics of Topological Magnetic Solitons: Experiment and Theory* (Springer–Verlag, Berlin, 1994).

[5] A. M. Kosevich, B. A. Ivanov, and A. S. Kovalev, Physica D **3**, 363 (1981); Phys. Rep. **194**, 117 (1990).

[6] V. G. Bar'yakhtar and B. A. Ivanov, Sov. Sci. Rev., Sect. A **16**, 3 (1993).

[7] T. H. Skyrme, Proc. R. Soc. London, Ser. A **260**, 127 (1961).

[8] D. L. Huber, Phys. Rev. B **26**, 3758 (1982).

[9] V. L. Berezinskii, Sov. Phys. JETP **34**, 610 (1972).

[10] J. M. Kosterlitz and D. J. Thouless, J. Phys. C **6**, 1181 (1973).

[11] *Advanced Magnetic Nanostructures*, in edited by D. J. Sellmyer and R. Skomski (Springer, Berlin, 2006).

[12] J. C. Collins and W. J. Zakrzewski, arXiv:0809.0459 (unpublished).

[13] M. G. Alford and G. Good, Phys. Rev. B **78**, 024510 (2008).

[14] E. Babaev and M. Speight, Phys. Rev. B **72**, 180502(R) (2005).

[15] E. Babaev, arXiv:0901.4380 (unpublished).

[16] R. Balakrishnan and R. Dandoloff, Phys. Lett. A **303**, 273 (2002).

[17] A. Saxena and R. Dandoloff, Phys. Rev. B **66**, 104414 (2002).

[18] R. Dandoloff and A. Saxena, Eur. Phys. J. B **29**, 265 (2002).

[19] F. Waldner, J. Magn. Magn. Mater. **31-34**, 1203 (1983); **54-57**, 873 (1986); **104-107**, 793 (1992).

[20] C. E. Zaspel, T. E. Grigereit, and J. E. Drumheller, Phys. Rev. Lett. **74**, 4539 (1995); K. Subbaraman, C. E. Zaspel, and J. E. Drumheller, *ibid.* **80**, 2201 (1998); C. E. Zaspel and J. E. Drumheller, Int. J. Mod. Phys. B **10**, 3649 (1996).

[21] A. A. Belavin and A. M. Polyakov, JETP Lett. **22**, 245 (1975).

[22] C. Moutafis, S. Komineas, C. A. F. Vaz, J. A. C. Bland, and P. Eames, Phys. Rev. B **74**, 214406 (2006).

[23] R. H. Hobart, Proc. Phys. Soc. London **82**, 201 (1963).

[24] G. H. Derrick, J. Math. Phys. **5**, 1252 (1964).

[25] G. M. Wysin, Phys. Rev. B **71**, 094423 (2005).

[26] L. Cincio, J. Dziarmaga, M. M. Rams, and W. H. Zurek, Phys. Rev. A **75**, 052321 (2007).

[27] V. S. L'vov, *Nonlinear Spin Waves* (Nauka, Moscow, 1987), in Russian.

[28] A. V. Kimel, A. Kirilyuk, A. Tsvetkov, R. V. Pisarev, and Th. Rasing, Nature (London) **429**, 850 (2004).

[29] A. V. Kimel, A. Kirilyuk, P. A. Usachev, R. V. Pisarev, A. M. Balbashov, and Th. Rasing, Nature (London) **435**, 655 (2005).

[30] N. S. Manton, Ann. Phys. **256**, 114 (1997).

[31] B. A. Ivanov, A. Yu. Merkulov, V. A. Stephanovich, and C. E. Zaspel, Phys. Rev. B **74**, 224422 (2006).

[32] B. A. Ivanov and V. A. Stephanovich, Sov. Phys. JETP **64**, 376 (1986).

[33] B. A. Ivanov and G. M. Wysin, Phys. Rev. B **65**, 134434 (2002).

[34] The models with $A_\nu<0$ can be constructed, in principle, considering different exotic types of exchange interactions. Such consideration, however, is beyond the scope of present paper.

[35] S. Coleman, Nucl. Phys. B **262**, 263 (1985).

[36] R. A. Leese, Nucl. Phys. B **366**, 283 (1991).

[37] I. S. Gradshteyn and I. M. Ryzhik, *Table of Integrals, Series, and Products* (Academic, New York, 1980).

[38] V. P. Voronov, B. A. Ivanov, and A. M. Kosevich, Sov. Phys. JETP **57**, 1303 (1983).

[39] Ar. Abanov and V. L. Pokrovsky, Phys. Rev. B **58**, R8889 (1998).